

Collective motion of polar active particles on a sphere

Yi Chen(陈奕), Jun Huang(黄竣), Fan-Hua Meng(孟繁华), Teng-Chao Li(李腾超), and Bao-Quan Ai(艾保全)
Citation: Chin. Phys. B, 2021, 30 (**10**): 100510. DOI: 10.1088/1674-1056/abfccf
Journal homepage: http://cpb.iphy.ac.cn; http://iopscience.iop.org/cpb

What follows is a list of articles you may be interested in

Nonlinear dynamics of cell migration in anisotropic microenvironment

Yanping Liu(刘艳平), Da He(何达), Yang Jiao(焦阳), Guoqiang Li(李国强), Yu Zheng(郑钰), Qihui Fan(樊琪慧), Gao Wang(王高), Jingru Yao(姚静如), Guo Chen(陈果), Silong Lou(娄四龙), and Liyu Liu(刘雳宇)
Chin. Phys. B, 2021, 30 (**9**): 090505. DOI: 10.1088/1674-1056/ac11d5

Stationary response of colored noise excited vibro-impact system

Jian-Long Wang(王剑龙), Xiao-Lei Leng(冷小磊), and Xian-Bin Liu(刘先斌)
Chin. Phys. B, 2021, 30 (**6**): 060501. DOI: 10.1088/1674-1056/abf12a

Surface active agents stabilize nanodroplets and enhance haze formation

Yunqing Ma(马韵箐), Changsheng Chen(陈昌盛), and Xianren Zhang(张现仁)
Chin. Phys. B, 2021, 30 (**1**): 010504. DOI: 10.1088/1674-1056/abca1e

Directed transport of coupled Brownian motors in a two-dimensional traveling-wave potential

Wei-Xia Wu(吴魏霞), Zhi-Gang Zheng(郑志刚), Yan-Li Song(宋艳丽), Ying-Rong Han(韩英荣), Zhi-Cheng Sun(孙志成), Chen-Pu Li(李晨璞)
Chin. Phys. B, 2020, 29 (**9**): 090503. DOI: 10.1088/1674-1056/ab99b7

Homoclinic orbits in three-dimensional Shilnikov-type chaotic systems

Feng Jing-Jing, Zhang Qi-Chang, Wang Wei, Hao Shu-Ying
Chin. Phys. B, 2013, 22 (**9**): 090503. DOI: 10.1088/1674-1056/22/9/090503

Collective motion of polar active particles on a sphere*

Yi Chen(陈奕)[1,2], Jun Huang(黄竣)[1,2], Fan-Hua Meng(孟繁华)[1,2], Teng-Chao Li(李腾超)[1,2,†], and Bao-Quan Ai(艾保全)[1,2,‡]

[1] *Guangdong Provincial Key Laboratory of Quantum Engineering and Quantum Materials, School of Physics and Telecommunication Engineering, South China Normal University, Guangzhou* 510006, *China*
[2] *Guangdong–Hong Kong Joint Laboratory of Quantum Matter, South China Normal University, Guangzhou* 510006, *China*

(Received 4 February 2021; revised manuscript received 21 April 2021; accepted manuscript online 29 April 2021)

Collective motion of active particles with polar alignment is investigated on a sphere. We discussed the factors that affect particle swarm motion and define an order parameter that can show the degree of particle swarm motion. In the model, we added a polar alignment strength, along with Gaussian curvature, affecting particles swarm motion. We find that when the force exceeds a certain limit, the order parameter will decrease with the increase of the force. Combined with our definition of order parameter and observation of the model, the reason is that particles begin to move side by side under the influence of polar forces. In addition, the effects of velocity, rotational diffusion coefficient, and packing fraction on particle swarm motion are discussed. It is found that the rotational diffusion coefficient and the packing fraction have a great influence on the clustering motion of particles, while the velocity has little influence on the clustering motion of particles.

Keywords: clustering motion of Brownian particles, polar active particles, sphere

PACS: 05.10.Gg, 05.40.Jc, 05.20.–y, 05.60.–k **DOI:** 10.1088/1674-1056/abfccf

1. Introduction

In nature, the collective motion of various living systems (for example, bird flocks,[1] fish schools,[2] bacterial colonies,[3] and mixtures of motor and cytoskeletal proteins,[4]) and the synthesis of slender living particle swarms have interesting common features, such as swirling patterns and swarming-related to the alignment of motion with their neighbors.[5] Vicsek *et al.* proposed an agent-based minimal model for flocking, accounting for the interplay between fluctuations and simultaneous interactions of multiple agents.[6] On the basis of these, there have been several works modeling the motion of micrometric on simple curved surface like sphere. Sanchez *et al.*[7] constructed a model of active particles confined to move on a sphere. Sknepnek carried out relevant research on the movement of active entities on the surface, and Henkes carried out computational research on the interaction of active particles moving on the sphere.[8] Along the same line, Bruss *et al.*[9] found the steady state profile of a flock on a sphere and on a catenoid, as well as topological modes due to curvature and activity in the system. Apaza and Sandoval[10] generalized the dynamics of active Brownian particles (ABPs) moving on the surface of a sphere by adding both translational and rotational Brownian motion. In addition, Janssen *et al.*[11] studied the motion of self-propelled particles (spheres and rods) on a sphere, and for various particle densities. A theoretical study on the dynamics of active particles performing rotational Brownian motion on curved surfaces has also been presented by Fily *et al.*[12] Cui *et al*. proposed a strategy for separating micro-suspents by using micro-suspents to surf on the substrate chemical wave front.[13] Chen *et al*. found that new collective dynamics and structures appeared when the dimer's translational and rotational self-propulsion occurred simultaneously,[14] and made it possible for the chemical self-propulsion motor to operate in an active chemical medium far from equilibrium.[15] Shi *et al.* found that the self-organization pattern of cortical microtubules in plant cells can be regulated by controlling the assembly dynamics of individual microtubules.[16] These studies provide more possibilities for our theoretical research.

Beyond swarming, self-propelled particles (SPPs) also form dense clusters via motility-induced phase separation, whereby SPPs phase separate into coexisting dense and dilute phases.[17,18] When we observe the motion of particles on a curved surface, the existence of inherent surface curvature disrupts the local order, resulting in a phenomenon different from that in a two-dimensional plane.[11,19–34] It has been proved that the degree of phase separation of SPPs on the surface is largely caused by the microgroup effect and depended on the gaussian curvature of the closed surface nonlinearly.[9] Focus-

*Project supported in part by the National Natural Science Foundation of China (Grant Nos. 12075090 and 12005066), the Science and Technology Program of Guangzhou (Grant No. 2019050001), the Natural Science Foundation of Guangdong Province, China (Grant No. 2017A030313029), and the Major Basic Research Project of Guangdong Province, China (Grant No. 2017KZDXM024).

†Corresponding author. E-mail: tengchaoli@m.scnu.edu.cn
‡Corresponding author. E-mail: aibq@scnu.edu.cn

© 2021 Chinese Physical Society and IOP Publishing Ltd

ing on the case of self-propelled particles confined to the surface of a sphere, they found that for high curvature, particles converge to a common orbit to form symmetry-breaking microswarms. In the Vicsek model, particles are point like and align instantaneously. The model can be extended to include particle volume which has not been considered before, but its effects remain poorly understood, especially at high densities. In this paper, we discussed the motion of Brownian particles on a sphere with a combination of short-range repulsion and angular diffusion. In the model, we added a polar alignment strength that affects particles motion, along with gaussian curvature, affecting particle swarm motion.

2. Model and methods

We consider that N spherical particles of diameter σ are confined to a sphere surface of radius R. The dynamics of particle i is described by the position $\boldsymbol{r}_i \equiv (x_i, y_i, z_i)$ of its center and the orientation $\boldsymbol{n}_i$. The particle velocity v_0 and the direction $\boldsymbol{n}_i$ are constrained at each point in the tangent plane. The surface of the sphere is algebraically described by $g(\boldsymbol{r}_i) = 0$, where

$$g(\boldsymbol{r}_i) = x_i^2 + y_i^2 + z_i^2 - R^2.$$

We assume translational and rotational diffusion to be independent and translational diffusion to be negligibly small, so that the limit of small persistence lengths exists in the model effectively. In the overdamped limit, the dynamics of particle i are described by the following Langevin equations with holonomic constraint:[8,20,22]

$$\frac{\mathrm{d}\boldsymbol{r}_i}{\mathrm{d}t} = v_0\boldsymbol{n}_i + \mu\left[\sum_{j\neq i}\boldsymbol{F}_{ij} - G(\boldsymbol{r}_i)^{\mathrm{T}}\lambda_i\right], \tag{1}$$

where $\boldsymbol{F}_{ij}$ is the short-range nonactive two-body force and μ is the mobility. $G(\boldsymbol{r}) = \bigtriangledown_r g(\boldsymbol{r})$ is the gradient of $g(\boldsymbol{r})$. λ is the Lagrange multiplier which is determined by the RATTLE algorithm.[35] Note that $g(\boldsymbol{r})$ can be interpreted as a potential, and the constraint trajectories will then lie on the isopotential surface with potential value 0. Therefore, there exists an effective force $G(\boldsymbol{r}_i)^{\mathrm{T}}\lambda_i$ that penalizes any deviations from the isopotential surface, which prevents particles falling down from the surface.

Particles interact through short ranged soft repulsive forces $\boldsymbol{F}_{ij} = k(2\sigma - r_{ij})\hat{\boldsymbol{r}}_{ij}$ if particles overlap ($r_{ij} < 2\sigma$), and $\boldsymbol{F}_{ij} = 0$ otherwise. As one can see in Fig. 1, $r_{ij} = |\boldsymbol{r}_i - \boldsymbol{r}_j|$ is the distance between particle i and particle j and $\hat{\boldsymbol{r}}_{ij} = (\boldsymbol{r}_i - \boldsymbol{r}_j)/r_{ij}$. Here k is the spring constant. In order to mimic hard particles, we use a larger value for the product of spring constant and mobility μk, thus ensuring that particle overlaps decay quickly.

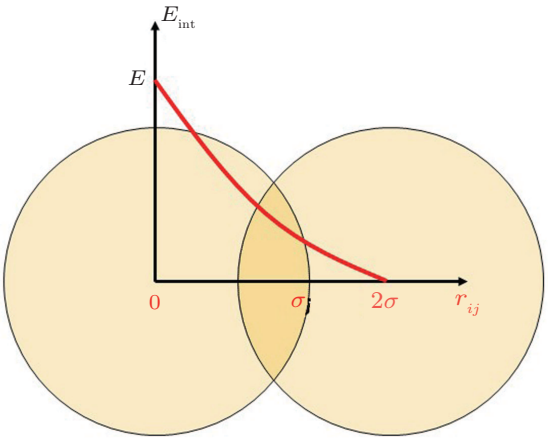


Fig. 1. Particles interact via a short-range soft potential E_{int}, which is finite for any value of r_{ij}.

In order to fully describe motion of the particles, we need to also specify dynamics for the internal degree of freedom, *i.e.*, the direction vector $\boldsymbol{n}_i$. Usually, the dynamics of $\boldsymbol{n}_i$ contains two contributions to the torque:[22] (i) polar alignment of neighboring directors and (ii) polar alignment of the director $\boldsymbol{n}_i$ with the direction of its own velocity. The second alignment in our model takes effect only when the activity of particles is very low. Therefore, we only consider the first polar alignment. So the XY-like angular dynamics on the sphere is given by[8]

$$\frac{\mathrm{d}\boldsymbol{n}_i}{\mathrm{d}t} = \left[\boldsymbol{P}_N(\hat{\boldsymbol{r}}_i, -J\sum_j \boldsymbol{n}_i \times \boldsymbol{n}_j) + \xi_i(t)\right](\hat{\boldsymbol{r}}_i \times \boldsymbol{n}_i), \tag{2}$$

where $\xi_i(t)$ is a scalar delta-correlated angular noise with distribution $\langle \xi_i(t)\xi_j(t')\rangle = D_{\mathrm{r}}\sigma_{ij}\sigma(t-t')$, and D_{r} is the rotational diffusion constant. The summation in Eq. (2) is carried over all neighbors within a 4.0σ cut off radius. Where J is polar alignment strength and we only consider the ferromagnetic case ($J > 0$) and $\hat{\boldsymbol{r}}_i$ is the local surface normal. The $\boldsymbol{P}_N$ is the normal projection of a vector on the unit normal to the tangent plane as $\boldsymbol{P}_N(\hat{\boldsymbol{N}}_i, \boldsymbol{a}) = (\boldsymbol{a}\cdot\hat{\boldsymbol{N}}_i)$. The orientational order of active particles on a sphere can be characterized by the polar order parameter

$$P = \frac{1}{N}\left|\sum_i^N \boldsymbol{r}_i \times \boldsymbol{n}_i\right|.$$

Active particles move in any direction with equal probability when $P \to 0$, while active particles move together along a circulating ring when $P \to 1$. We define the ratio between the area occupied by particles and the total available area as the packing fraction $\varphi = N\pi(\sigma/2)^2/4\pi R^2$.

3. Results and discussion

In our simulations, equation (1) has been numerically solved by using RATTLE discretization.[35] Particles are constrained to the curved surface by projecting the positions and

force vectors back onto the local tangent plane after every time step. Equation (2) has been integrated numerically, the torques were projected onto the surface normal at $\boldsymbol{r}_i$, and finally, $\boldsymbol{n}_i$ was rotated by a random angle around the same normal.[36] The integration step time $\Delta t = 0.01$ and the total integration time was more than 10^6. The stochastic averages were obtained as ensemble averages over 300 trajectories with random initial conditions. Unless otherwise noted, our simulations were under the parameter sets: $\mu k = 50$, $\sigma = 0.5$, $\varphi = 0.12$. We tested that the presented results are robust against reasonable changes in these parameters. In the following, we explore the collective behavior of particles by the rotational diffusion coefficient D_{r}, the polar alignment strength J, and the self-propelled velocity v_0.

Figure 2 simulates the motion of particles on the sphere. When the radius of sphere and packing fraction remain unchanged, with the increase of the polar alignment strength J, the collective motion of particles gradually changes from disorder to order. When the polar alignment strength $J = 0.001$, as shown in Fig. 2(a), the active particles move randomly on the sphere. When the polar alignment strength $J = 0.02$, as shown in Fig. 2(b), the active particles exhibit a small range of clustered and ordered collective motion. When the polar alignment strength $J = 5$, as shown in Fig. 2(c), the active particles move in an ordered group around the equator.

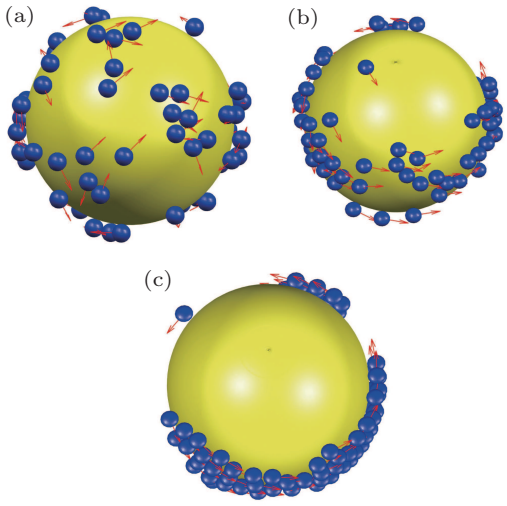


Fig. 2. The schematic motion of particles on a sphere when the radius of sphere and packing fraction remain unchanged (the radius of sphere $R = 6$ and the packing fraction $\varphi = 0.12$). (a) When the polar alignment strength $J = 0.001$, the active particles move randomly on the sphere. (b) When the polar alignment strength $J = 0.06$, the active particles have a small range of clustered and ordered collective motion. (c) When the polar alignment strength $J = 5$, the active particles move in ordered groups around the equator.

Figure 3 shows the order parameter P as the ratio of the radius of the sphere to the diameter of the particle R/σ for different values of the polar alignment strength J. When the polar alignment strength $J = 0$ (represented by the black line), the order of particles decreases as the radius of the sphere increases. In this case, the collective behavior of the particles is only related to the gaussian curvature.[9] The larger the polar alignment strength J is, the larger the order parameter P is, and the smaller R/σ is, the larger the order parameter P is. Therefore, there is a competitive relationship between the polar alignment strength J and R/σ. When $0 < J < 1$, due to the influence of the polar alignment strength J, the order parameter P of particle motion decreases first and then increases with the increase of R/σ. As can be seen from the Fig. 3, with the increase of the polar alignment strength J, the curvature has less influence on the collective motion of particles. When $J > 1$, the polar alignment strength J becomes the main factor affecting the collective motion of particles.

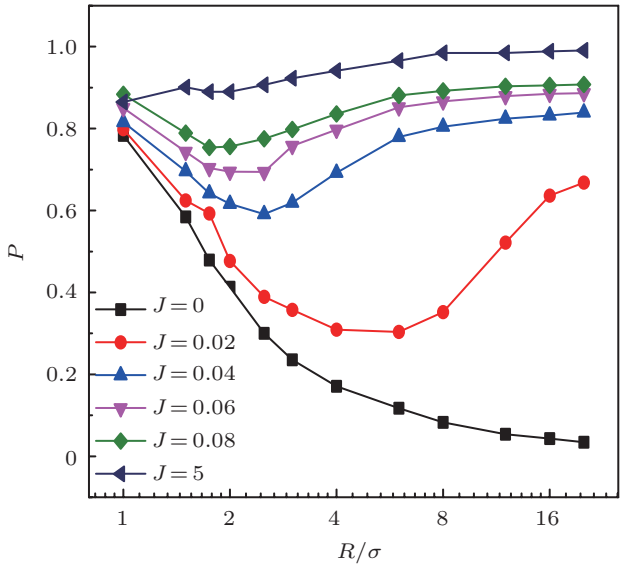


Fig. 3. The order parameter P *versus* the ratio of the radius of the sphere to the diameter of the particle R/σ for different J at $\varphi = 0.12$, $D_{\mathrm{r}} = 0.01$, and $v_0 = 1$.

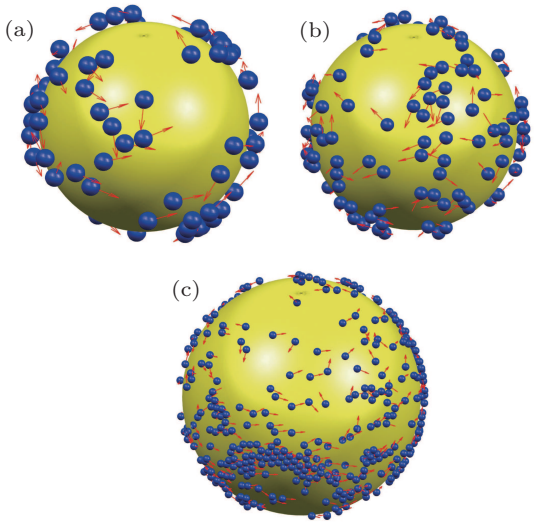


Fig. 4. The collective motion of particles when the polar alignment strength $J = 0.02$. (a) The order parameter $P = 0.30$ with the radius of sphere $R = 6$. (b) The order parameter $P = 0.36$ with the radius of sphere $R = 8$. (c) The order parameter $P = 0.629$ with the radius of sphere $R = 16$.

When the polar alignment strength $J = 0.02$, we change the radius of the sphere R. As can be seen from Fig. 4, with the decrease of the gaussian curvature (in a sphere, the Gaussian curvature is the reciprocal of the radius of the sphere) of the sphere, the collective motion of particles gradually changes from disorder to order. When the radius of sphere $R = 6$, the order parameter $P = 0.30$, and the active particles move randomly in small clusters on the sphere. When the radius of sphere $R = 8$, the order parameter $P = 0.36$, and the active particles move in an ordered manner with small clusters; when the radius of sphere $R = 16$, the order parameter $P = 0.629$, and the active particles move in an ordered manner with clusters.

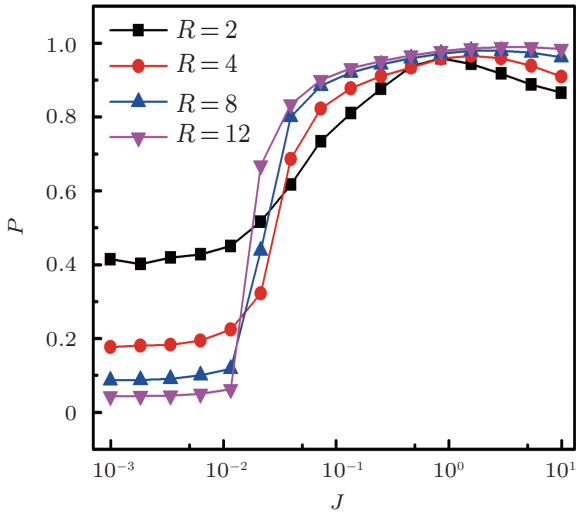


Fig. 5. The order parameter P *versus* the polar alignment strength J for different R at $\varphi = 0.12$, $D_r = 0.01$, and $v_0 = 1$.

The collective motion of particles is affected by the radius R and the polar alignment strength J. Figure 5 shows the order parameter P corresponding to the continuously changing the polar alignment strength J when the radius R is different. When the radius R remains unchanged, the order parameter P increases with the increase of the polar alignment strength J and eventually approaches 1, that is, the collective motion of particles is in order. When the polar alignment strength J is relatively small ($J < 0.01$), the main factor affecting the collective motion of particles is the size of radius, that is, the order parameter P of particles decreases with the increase of the radius R. When $0.01 < J < 1$, the influence of the polar alignment strength J on the collective motion of particles is dominant, and the order parameter P increases with the increase of the polar alignment strength J. In addition, it can be found that the larger the radius R of the sphere, the greater the influence of the polar alignment strength J on the collective motion of the particle. This is because the larger the gaussian curvature is, the greater the constraint on the collective motion of the particle is. In particular, it can be seen from Fig. 5, when $1 < J < 10$, P decreases as J increases. In this case, the decrease of the order parameter P is caused by the definition of the order parameter. As one can see from the definition of P, when all the particles move in a circle around the equator of the sphere, P approaches 1, as shown in Fig. 6(a). When J is too large, particles will cluster together and move around the equator, and particles above or below the equator will lower the value of P, as shown in the Fig. 6(b). Furthermore, we have a phase diagram P of J and R, as shown in Fig. 7, and the order parameter P increases as the color goes from blue to red.

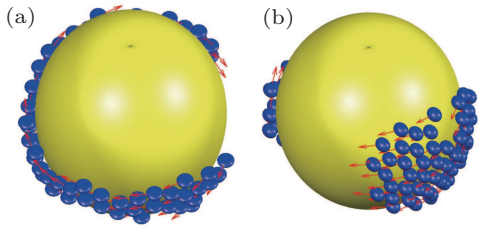


Fig. 6. Different states of motion of particles at $\varphi = 0.12$, $D_r = 0.01$, $v_0 = 1$, and $R = 6$. (a) The particles move in long chains around the equator. (b) Particles clumped together and moved around the equator.

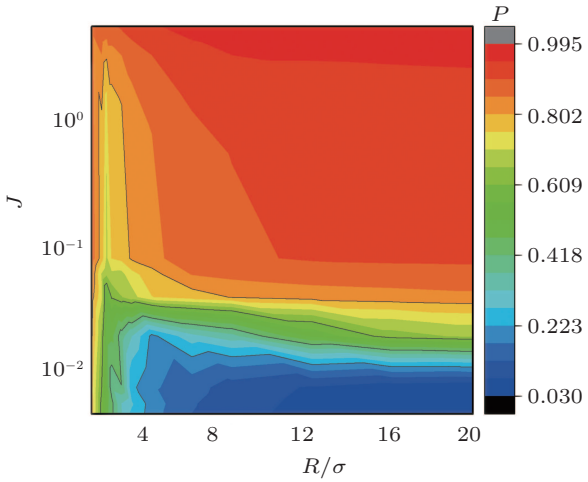


Fig. 7. The phase diagram of P *versus* J for different R at $\varphi = 0.12$, $D_r = 0.01$, and $v_0 = 1$.

In addition, figure 8 shows the effects of the polar alignment strength J and velocity of particles v_0 on the order parameter P. As shown in Fig. 8(a), we observed the change of P with the continuous change of v_0 in the case of different J. The function of J is to make particles move collectively, and the function of v_0 is to disperse particles, so there is a competitive relationship between the two on the influence of the collective motion of particles. When $0 < J < 0.02$, the value of J is too small for the particles to gather together for collective motion, so even if v_0 increases, P almost does not change. When $0.02 < J < 0.1$, the effect of J is dominant when v_0 is small, so the collective motion of particles has a certain order. Because the larger v_0 is, the larger distance the particle moves in each step, which makes it difficult for the particles to move collectively. Therefore, the P of the particles decreases

with the increase of v_0. When $0.1 < J < 10$, the role of J is dominant, thus P does not change much in the range of v_0 we take. It is worth noting that, combined with Fig. 5, although P changes rapidly from $J = 0.01$ to $J = 0.05$, its change is still continuous rather than abrupt, since the order parameter P still changes gradually when we make J denser. Figure 8(b) shows the change of P with continuous change of v_0 when R is different. As can be seen from the figure, the velocity of particles has little influence on the collective motion of particles, and the larger J and R are, the more ordered are the particles. At the same time, we also observed the influence of the polar alignment strength J and rotational diffusion coefficient D_r on the order parameter P.

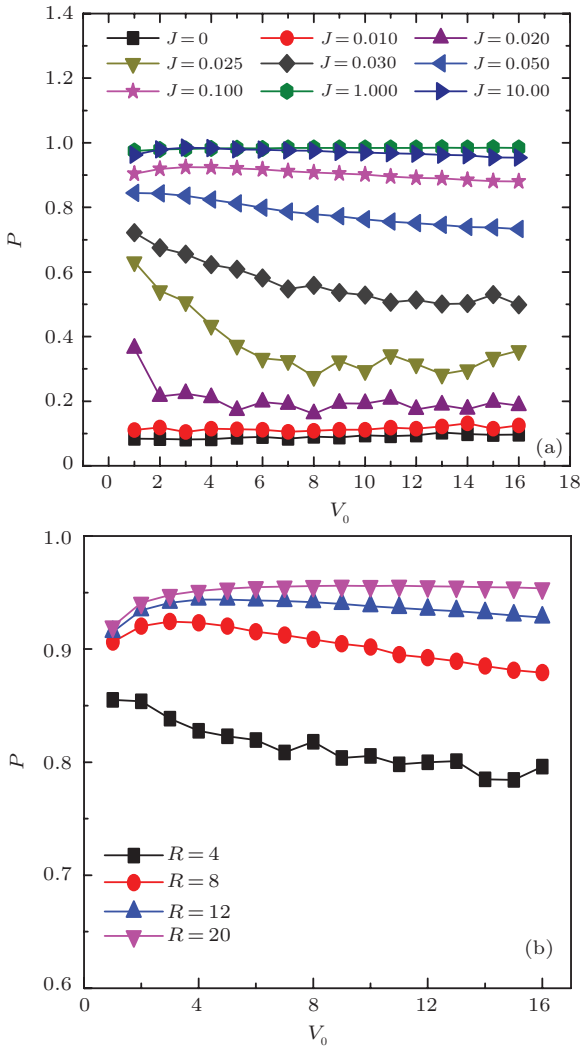


Fig. 8. (a) P *versus* v_0 of the particles for different J at $\varphi = 0.12$, $D_r = 0.01$, and $R = 8$. (b) P *versus* v_0 of the particles for different R at $\varphi = 0.12$, $D_r = 0.01$, and $J = 0.1$.

Figure 9(a) shows the continuous change of P with D_r at different J. As can be seen from the figure, the higher the rotational diffusion coefficient is, the more disordered are the particles. This is because the higher the rotational diffusion coefficient is, the more active particles will be. The larger J is, the less influence the rotational diffusion coefficient has on the collective motion of particles. In other words, the larger J is, the larger the rotational diffusion coefficient is needed to break the ordered motion of particles. While figure 9(b) shows the change of P when D_r increases continuously with different R. Obviously, the order parameter P decreases as the rotational diffusion coefficient D_r increases, and the effect of the rotational diffusion coefficient D_r on particles increases with the increase of the radius of the sphere R.

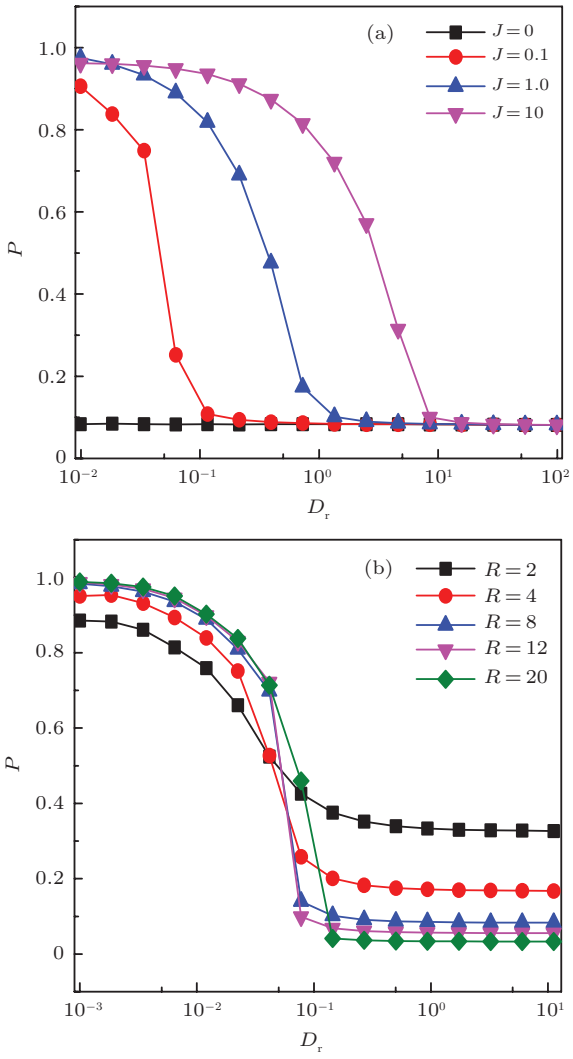


Fig. 9. (a) The order parameter P *versus* D_r of the particles for different J at $\varphi = 0.12$, $v_0 = 1$, and $R = 8$. (b) The order parameter P *versus* D_r of the particles for different R at $\varphi = 0.12$, $v_0 = 1$, and $J = 0.1$.

At last, we observed the change of P under different R and φ. It can be seen from Fig. 10 that when φ is small ($\varphi < 0.3$), the influence of different radius R on P is constant under the same φ. When φ is relatively large ($\varphi > 0.3$), under the same φ, the larger the spherical radius, the larger the P. Thus it can be seen that under the same φ, both the radius R and the packing fraction φ influence the effect of the polar alignment strength J. Obviously, the bigger R is, the more space particles move, the stronger the effect of J is.

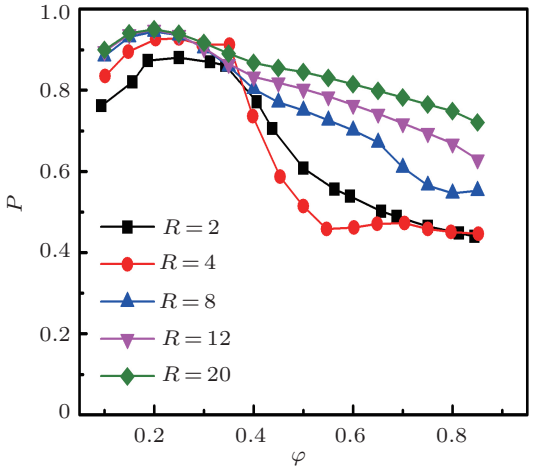


Fig. 10. The order parameter P *versus* the packing fraction φ of the particles for different R at $D_r = 0.01$, $v_0 = 1$, and $J = 0.1$.

4. Concluding remarks

In conclusion, we discussed the motion of active particles on a sphere under the influence of the polar alignment strength J and the radius of sphere R. Particles moving on the sphere are affected by the radius of sphere R and the polar alignment strength J, and they compete with each other. When J increases, the influence of curvature on the collective motion of particles will decrease. When $J > 1$, J becomes the main factor affecting the collective motion of particles. In addition, we also observed the particle clustering under different D_r and different particle velocities v_0. From the results, the velocity of active particles has little effect on the motion of particle clusters, and the rotational diffusion coefficient of particles will affect the motion of particles clusters. A relatively large rotational diffusion coefficient is not conducive to the formation of ordered motion of particles. At last, we also discussed the change of P under different R and φ. Under the influence of the same J, particles with smaller gaussian curvature and smaller packing fraction are more likely to form an ordered motion of clustering.

References

[1] Cavagna A, Cimarelli A, Giardina I, Parisi G, Santagati R, Stefanini F and Viale M 2010 *Proc. Natl. Acad. Sci. USA* **107** 11865

[2] Tunstrom K, Katz Y, Ioannou C C, Huepe C, Lutz M J and Couzin I D 2013 *PLoS Computational Biology* **9**

[3] Lushi E, Wioland H and Goldstein R E 2014 *Proc. Natl. Acad. Sci. USA* **111** 9733

[4] Giomi L, Bowick M J, Ma X and Marchetti M C 2013 *Phys. Rev. Lett.* **110** 228101

[5] Vicsek T and Zafeiris A 2012 *Phys. Rep.* **517** 71

[6] Vicsek T, Czirók A, Ben-Jacob E, Cohen I and Shochet O 1995 *Phys. Rev. Lett.* **75** 1226

[7] Sanchez T, Chen D T, DeCamp S J, Heymann M and Dogic Z 2012 *Nature* **491** 431

[8] Sknepnek R and Henkes S 2015 *Phys. Rev. E* **91** 022306

[9] Bruss I R and Glotzer S C 2017 *Soft Matter* **13** 5117

[10] Apaza L and Sandoval M 2017 *Phys. Rev. E* **96** 022606

[11] Janssen L M C, Kaiser A and Löwen H 2017 *Sci. Rep.* **7** 5667

[12] Fily Y, Baskaran A and Hagan M F 2017 *Eur. Phys. J. E* **40** 61

[13] Cui R F, Chen Q H and Chen J X 2020 *Nanoscale* **12** 12275

[14] Chen J X, Yuan R, Cui R and Qiao L Y 2021 *Nanoscale* **13** 1055

[15] Chen J X, Chen Y G and Kapral R 2018 *Adv. Sci.* **5** 1800028

[16] Shi X Q and Ma Y Q 2010 *Proc. Natl. Acad. Sci. USA* **107** 11709

[17] Fily Y and Marchetti M C 2012 *Phys. Rev. Lett.* **108** 235702

[18] Stenhammar J, Tiribocchi A, Allen R J, Marenduzzo D and Cates M E 2013 *Phys. Rev. Lett.* **111** 145702

[19] Keber F C, Loiseau E, Sanchez T, DeCamp S J, Giomi L, Bowick M J, Marchetti M C, Dogic Z and Bausch A R 2014 *Science* **345** 1135

[20] Alaimo F, Köhler C and Voigt A 2017 *Sci. Rep.* **7** 5211

[21] Praetorius S, Voigt A, Wittkowski R and Löwen H 2018 *Phys. Rev. E* **97** 052615

[22] Henkes S, Marchetti M C and Sknepnek R 2018 *Phys. Rev. E* **97** 042605

[23] Ellis P W, Nayani K, McInerney J P, Rocklin D Z, Park J O, Srinivasarao M, Matsumoto E A and Fernandez-Nieves A 2018 *Phys. Rev. Lett.* **121** 247803

[24] Shankar S, Ramaswamy S, Marchetti M C and Bowick M J 2018 *Phys. Rev. Lett.* **121** 108002

[25] Norton M M, Baskaran A, Opathalage A, Langeslay B, Fraden S, Baskaran A and Hagan M F 2018 *Phys. Rev. E* **97** 012702

[26] Ehrig S, Ferracci J, Weinkamer R and Dunlop J W C 2017 *Phys. Rev. E* **95** 062609

[27] Shankar S, Bowick M J and Marchetti M C 2017 *Phys. Rev. X* **7** 031039

[28] Mickelin O, Slomka J, Burns K J, Lecoanet D, Vasil G M, Faria L M and Dunkel J 2018 *Phys. Rev. Lett.* **120** 164503

[29] Fonda P, Rinaldin M, Kraft D J and Giomi L 2018 *Phys. Rev. E* **98** 032801

[30] Pearce D J G, Ellis P W, Fernandez-Nieves A and Giomi L 2019 *Phys. Rev. Lett.* **122** 168002

[31] Castro-Villarreal P and Sevilla F J 2018 *Phys. Rev. E* **97** 052605

[32] Giomi L 2015 *Phys. Rev. X* **5** 031003

[33] Yan W and Brady J F 2018 *Soft Matter* **14** 279

[34] Ai B Q, Zhu W J and Liao J J 2019 *New J. Phys.* **21** 093041

[35] Leimkuhler B and Reich S 2004 *Simulating Hamiltonian Dynamics* (Cambridge: Cambridge University Press)

[36] Ellis P W, Nayani K, McInerney J P, Rocklin D Z, Park J O, Srinivasarao M, Matsumoto E A and Fernandez-Nieves A 2018 *Phys. Rev. Lett.* **121** 247803